Geoderma 342 (2019) 106–108

Contents lists available at ScienceDirect

Geoderma

journal homepage: www.elsevier.com/locate/geoderma

XRF-measured rubidium concentration is the best predictor variable for estimating the soil clay content and salinity of semi-humid soils in two catenas

Tibor Tóth*, Zsófia Adrienn Kovács, Márk Rékási

Institute for Soil Sciences and Agricultural Chemistry, Centre for Agricultural Research of the Hungarian Academy of Sciences, Budapest II, Herman O. út 15, 1022, Hungary

ARTICLE INFO

Handling Editor: Alex McBratney

Keywords:
Sodicity
Salinity
Gamma dosimetry
X-ray fluorescence spectroscopy

ABSTRACT

When making management decisions regarding the conditions of the Great Hungarian Plain, it is important to consider the soil clay content and soil salinity. Because the soil moisture conditions vary from extremely dry to extremely wet throughout the year, this limits the use of electric methods. In this study, we looked for fast, independent techniques to estimate soil clay content and soil salinity. Gamma dosimetry and X-ray fluorescence spectroscopy (XRF) were tested and showed consistent values. In two contrasting transects: one passing from top of the dune to the valley (Sanddune-Valley), and another passing from an elevated non-sodic grassland to low sodic patches (Sodic), the XRF-measured rubidium concentration proved to be the best overall predictor of both soil clay content and salinity as it provided better correlations than gamma dosimetry. Pearson correlation coefficients indicated opposing tendencies between the rubidium concentration and the soil clay content and salinity in the transects, owing to distinct differences in the soil formations inside the transects. We suggest using XRF and not gamma dosimetry for the field estimation of soil clay content and salinity with portable devices.

In the conditions of semi-humid regions, soil clay content and salinity are important factors that can limit the agricultural use of soils and field instrumental techniques. Therefore, electric and electromagnetic methods usually are available for their estimation. Due to recurrent changing weather conditions, extremes of dry, wet or frozen conditions limit the use of the above-mentioned methods, which have the precondition of moist soil. In very dry soils, the relationship between field and laboratory-measured soil electrical conductivity is weak (Joshi et al., 2006). Most importantly, it is essential to make an accurate estimation of the soil salinity in the topsoil where the fluctuation of moisture is the greatest (Douaik et al., 2006). These methods are sensitive for both soil clay content and salinity and in nonsaline moist soils clay content is easily estimated. When salts are present in considerable but not too large amounts, differentiating between soil clay content and salinity is not possible (Sudduth et al., 2005). In this study, the 0.3–0.4 dS m^{-1} bulk soil electrical conductivity (ECa) values (Fig. 1) could be the result of the clay content being larger than 30%, or because of the low level of salinity. Such thresholds depend on all other affecting factors, such as soil moisture content, cation exchange capacity, texture, etc. (Rhoades et al., 1976; Friedman, 2005). Our objective was to find a quick field method capable of predicting the soil salinity and soil clay content independent of instantaneous moisture content.

Portable XRF (X-Ray Fluorescence Spectroscopy) devices are widely used for quick soil analyses to measure the concentration of a wide range of elements. Coupled with elemental concentrations, spectral data can be interpreted with respect to predicting soil properties (Zhang and Hartemink, 2018). Earlier studies demonstrated that soil element concentrations measured by XRF can be used to predict soil chemical and physical properties, analyse pedogenic processes or distinguish soil horizons (Weindorf et al., 2012). With this method, soil properties like pH, SOM or CEC can be estimated by the knowledge of soil element concentration data (Wang et al., 2015). For the study of the spatial and temporal variability of salinity, the single most important element is sodium, but portable XRF instruments are not capable of measuring it directly (Rousseau, 2001).

We used gamma-ray spectrometry with an external NaI(Tl) detector as an independent method of soil clay content estimation based on natural gamma radiation. Most gamma photons measured from soils are emitted from three typical radioactive isotopes: ^{40}K (ca 0.01% of all potassium), ^{232}Th and ^{238}U. Among them, K is most abundant in soils, with its concentration determined by geochemical, plant physiological, as well as agronomical conditions. Soil clay content has been proven to

* Corresponding author.
E-mail addresses: tibor@rissac.hu (T. Tóth), kovacs.zsofia@agrar.mta.hu (Z.A. Kovács), rekasi@rissac.hu (M. Rékási).

https://doi.org/10.1016/j.geoderma.2019.02.011
Received 28 June 2018; Received in revised form 4 February 2019; Accepted 4 February 2019

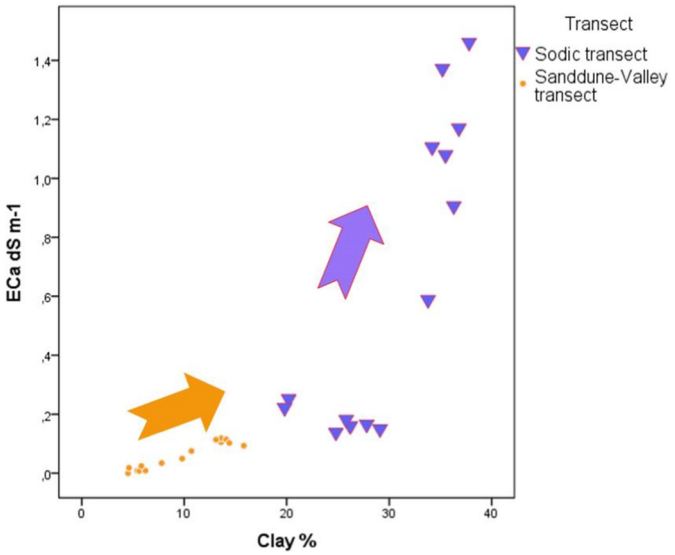

Fig. 1. Relationship between field-measured bulk soil electrical conductivity and soil clay content in the two studied transects. Arrows show the topographic descent direction of the respective transects.

strongly correlate with K content (Pracilio et al., 2006).

The two studied transects (catenas) were previously analysed for salinity and clay content and are routinely used as test sites of electric and electromagnetic instrumental measurements (Ristolainen et al., 2009). In our study there were great differences between the two 70–70 m long transects (Fig. 1).

The Sand dune-Valley transect on the outskirts of Kiskunlacháza, passes from the top of a coarse-textured sand dune (Arenosol) covered by trees, with a smooth, almost ideal transition to the cropped valley bottom, which is 1.6 m lower, where the clay and organic carbon contents are much higher (ca Chernozem). This transect is covered by a range of 4–16 clay % and 0–0.15 dS m^{-1} ECa in Fig. 1; low clay % and ECa values representing top-of-dune points, whereas high values belong to bottom-of-valley points.

The Sodic transect at Apaj passes from a nonsaline, nonsodic elevated point of tallgrass grassland (ca Chernozem) to the bottom of a natural, saline-sodic, semi-vegetated, and often waterlogged point 60 cm below (Solonetz). The transition is marked by distinct native vegetation patches of salt-tolerant plant species, having their characteristic micro-erosional mounds (10–15 cm height). Inside the transects, there is a strong correlation between salinity, alkalinity, organic carbon content, soil clay content, and these can accurately be predicted by electric and electromagnetic methods when moist, but also by elevation (Ristolainen et al., 2009). Since throughout the year soils vary from extremely dry to extremely wet, the accurate prediction is limited for spring and late autumn moist conditions. This transect is covered by a range of 26–40% clay and 0.18–1.5 dS m^{-1}, as shown in Fig. 1, where the low clay percentage and ECa values represent higher lying tallgrass points and high values belonging to bottom waterlogged points.

There were 15 soil sampling points along each transect, yielding one point every 5 m of the 70 m long transects. We carried out measurements using the gamma detector, XRF and an electromagnetic probe at the sampling points. XRF was used in duplicate measurements, directly on cleared soil surfaces with an Olympus Delta Premium portable XRF analyzer (featuring a 40 kV X-Ray tube and silicon drift detector) in Soilmode. The soil was then scanned at the sampling points for a duration of 60s in three-beam operation mode. Gamma dosimetry was performed using an InSpector™ 1000 Digital Hand-Held Multichannel Analyzer, noting the dose rate after placing it directly on the clear (cleaned of vegetation) surface for three minutes. The electromagnetic induction probe was placed on the soil surface in a vertical dipole orientation.

As reference laboratory data, clay fraction (< 0.002 mm) percentage of 0–20 cm was used (Ristolainen et al., 2009). Two outlier values (one soil clay content and one Rb concentration data) were discarded and the Pearson correlation coefficient was calculated between the measured data.

As Fig. 1. shows, an increase in soil clay content is indicated by larger ECa values in both transects. After a threshold value — ca 0.3 dS m^{-1} in this particular case — no longer the increase in the clay content, but the presence of soluble and adsorbed salt ions will result in very large conductivity values.

We checked the relationship between gamma dosimetry and XRF since potassium-40 is the most common radioactive isotope in typical soils; therefore, the major source of natural background soil gamma radiation. The theoretical relationship was proven by the case of the Sanddune-Valley transect because the Pearson correlation coefficient between dose rate and potassium concentration was 0.893** (** denotes $p < 0.01$), while in the case of Sodic transect it was 0.647**.

The three-minute-gamma-dose-rate was a good indicator of the laboratory-measured clay content inside the Sanddune-Valley transect (Pearson correlation coefficient 0.889**). However, the opposite was obtained in the Sodic transect, where the same Pearson correlation coefficient was −0.769**. This relationship is caused by the differences in mineral composition and the antagonism of sodium and potassium in sodic soils.

The abundance of several elements in soils is related to minerals that facilitate the instrumental estimation of clay content (Zhu et al., 2011). In our case, potassium concentration was approximately twice as much in the valley bottom in the Sanddune-Valley transect (1.94%) compared with the sand dune top (1.15%). On the contrary, in the Sodic transect, there was twice as much potassium in the nonsodic elevated position (1.92%) than in the sodic bottom position (0.96%). In the Sanddune-Valley transect, the dominance of coarse quartz and calcite particles at the coarsely-textured top of the transect, at the highest elevation (1.6 m compared to the valley bottom), certainly contributes to this significant difference. In the Sodic transect, the Na-montmorillonite dominates the low-lying sodic bottom, where K is displaced by sodium (Kuti et al., 2003).

The XRF-measured rubidium concentration, not potassium, was the overall best predictor variable in both transects of the bulk soil electrical conductivity and 0–20 cm soil clay content. The Pearson correlation coefficient between Rb and soil clay content was 0.974** in the Sanddune-Valley transect and −0.895** in Sodic transect (Fig. 2). The same coefficient between Rb and ECa was 0.926** in the Sanddune-Valley transect, and a correlation coefficient with similar statistical significance, but with an opposite sign of −0.925** was calculated in the Sodic transect.

XRF works through the excitation of the atoms and hence overperformed the short-time passive gamma dosimetry. Longer periods of measurement or larger detector volume (Triantafilis et al., 2013) could provide better results with the gamma dosimetry. The alkali metal Rb is an abundant element in the Earth's crust, although its measured concentration was < 1% of the potassium concentration. Geochemically it is closely related to potassium and due to the similar ionic radii, it can substitute potassium in minerals (Négrel et al., 2018). Since rubidium and K behave very similarly in solutions and on adsorptive surfaces, the results are not surprising. In the Sanddune-Valley transect, K overperformed Rb, with 0.939** and 0.984** correlation coefficient values with ECa and soil clay content, while the Sodic transect K was a less precise predictor, showing the same correlation coefficient −0.729** with both ECa and soil clay content. The Rb concentration might be a better predictor since it is less affected by plant uptake and agronomic practice (e.g., when applied as a fertilizer).

It is clear that the precision obtained during this study might be better had we indicated the endpoints of our reference transect with permanent marking pickets. Owing to the agronomic use of the lower

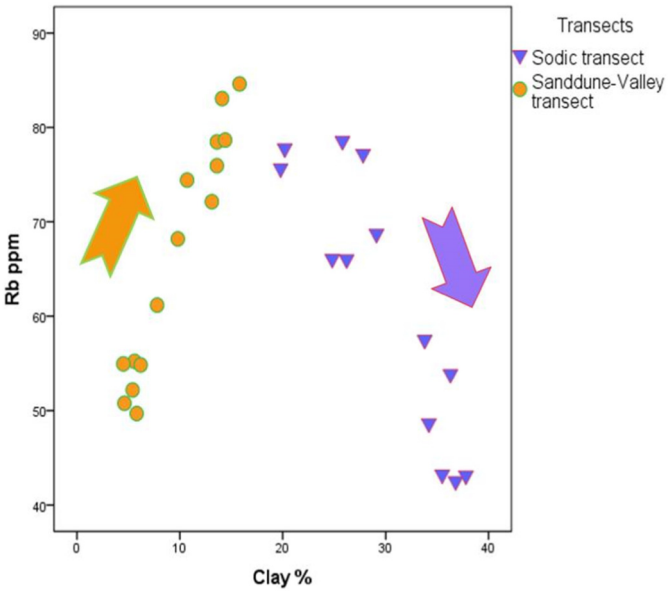

Fig. 2. Scattergram of soil clay content and XRF-measured rubidium concentration in two surface transects. Arrows show the topographic descent direction of the respective transects.

part of the Sanddune-Valley and the regular grazing and hay cutting of the Sodic transect area, it was not possible to use such pickets; therefore, the laboratory-measured salinity and soil clay content might have a component of spatial variability. A further factor causing scatter in the data is the varying support of the values. The field-measured parameters originated from a 7 cm auger hole diameter × 20 cm depth when analysed in the laboratory; a 2 × 2 cm square window × 0–15 cm depth when analysed with field gamma dosimetry (Viscarra Rossel et al., 2007); a 1 × 1 cm square window × 2 mm depth (two replicates inside one meter) when analysed in the field with XRF and a 100 cm width × 100 cm depth when analysed with electromagnetic induction probe.

In conclusion, the presence of soluble salts resulted in very distinctive catenas. Short-time (three minutes) field measurement with gamma dosimetry was less precise for the estimation of soil clay content ($r = 0.889^{**}$ in the Sanddune-Valley and -0.769^{**} in the Sodic transect) than the rubidium concentration measured by XRF ($r = 0.974^{**}$ in the Sanddune-Valley transect and -0.895^{**} in the Sodic transect). The same Rb concentration was a good predictor of soil bulk electrical conductivity ($r = 0.926^{**}$ in the Sanddune-Valley transect, and -0.925^{**} in the Sodic transect). XRF is suggested for estimating both soil salinity and clay content during short-time surveys.

Acknowledgements

This research is financed by the Hungarian National Research, Development and Innovation Office Foundation (Grant No. K 124290).

References

Douaik, A., Van Meirvenne, M., Tóth, T., 2006. Temporal stability of spatial patterns of soil salinity determined from laboratory and field electrical conductivity. Arid Land Res. Manag. 20, 1–13.

Friedman, S.P., 2005. Soil properties influencing apparent electrical conductivity: a review. Comput. Electron. Agric. 46 (1–3), 45–70.

Joshi, D., Tóth, T., Sári, D., 2006. Spatial variability of electrical conductivity of soils irrigated with brackish water in the arid region of Rajasthan, India. Ann. Arid Zone 45 (1), 9–17.

Kuti, L., Tóth, T., Kalmár, J., Kovács-Pálffy, P., 2003. Mineral composition of salt-affected soils and recent mineral formation in the neighborhood of Apajpuszta and Zab-szék. (in Hungarian). Agrokém. Talajt. 52, 275–285.

Négrel, P., Ladenberger, A., Reimann, C., Birke, M., the GEMAS Project Team, 2018. Distribution of Rb, Ga and Cs in agricultural land soils at European continental scale (GEMAS): implications for weathering conditions and provenance. Chem. Geol. 479, 188–203.

Pracilio, G., Adams, M.L., Smettem, K.R., Harper, R.J., 2006. Determination of spatial distribution patterns of clay and plant available potassium contents in surface soils at the farm scale using high resolution gamma ray spectrometry. Plant Soil 282 (1–2), 67–82.

Rhoades, J.D., Raats, P.A., Prather, R.J., 1976. Effects of liquid-phase electrical conductivity, water content, and surface conductivity on bulk soil electrical conductivity. Soil Sci. Soc. Am. J. 40, 651–655.

Ristolainen, A., Farkas, Cs, Tóth, T., 2009. Prediction of soil properties with field geoelectrical probes. Commun. Soil Sci. Plant Anal. 40, 555–565.

Rousseau, R.M., 2001. Detection limit and estimate of uncertainty of analytical XRF results. Rigaku J. 18 (2), 33–47.

Sudduth, K.A., Kitchen, N.R., Wiebold, W.J., Batchelor, W.D., Bollero, G.A., Bullock, D.G., Thelen, K.D., 2005. Relating apparent electrical conductivity to soil properties across the north-central USA. Comput. Electron. Agric. 46 (1–3), 263–283.

Triantafilis, J., Gibbs, I., Earl, N., 2013. Digital soil pattern recognition in the lower Namoi valley using numerical clustering of gamma-ray spectrometry data. Geoderma 192, 407–421.

Viscarra Rossel, R.A., Taylor, H.J., McBratney, A.B., 2007. Multivariate calibration of hyperspectral γ-ray energy spectra for proximal soil sensing. Eur. J. Soil Sci. 58 (1), 343–353.

Wang, D., Chakraborty, S., Weindorf, D.C., Li, B., Sharma, A., Paul, S., et al., 2015. Synthesized use of VisNIR DRS and XRF for soil characterization: total carbon and total nitrogen. Geoderma 243–244, 157–167.

Weindorf, D.C., Zhu, Y., McDaniel, P., Valerio, M., Lynn, L., Michaelson, G., Clark, M., LuPing, C., 2012. Characterizing soils via portable x-ray fluorescence spectrometer: 2. Spodic and albic horizons. Geoderma 189–190, 268–277.

Zhang, Y., Hartemink, A., 2018. Digital mapping of a soil profile. Eur. J. Soil Sci. https://doi.org/10.1111/ejss.12699.

Zhu, Y., Weindorf, D.C., Zhang, W., 2011. Characterizing soils using a portable X-ray fluorescence spectrometer: 1. Soil texture. Geoderma 167–68, 167–177.